ACCOUNTING FOR THE MISSING CARBON-SINK WITH THE CO_2-FERTILIZATION EFFECT

HAROON S. KHESHGI
Corporate Research Laboratories, Exxon Research and Engineering Company, Annandale, NJ 08801, U.S.A.

ATUL K. JAIN and DONALD J. WUEBBLES
Department of Atmospheric Sciences, University of Illinois, Urbana, IL 61801, U.S.A.

Abstract. A terrestrial–biosphere carbon-sink has been included in global carbon-cycle models in order to reproduce past atmospheric CO_2, ^{13}C and ^{14}C concentrations. The sink is of large enough magnitude that its effect on projections of future CO_2 levels should not be ignored. However, the cause and mechanism of this sink are not well understood, contributing to uncertainty of projections. The estimated magnitude of the biospheric sink is examined with the aid of a global carbon-cycle model. For CO_2 emissions scenarios, model estimates are made of the resulting atmospheric CO_2 concentration. Next, the response of this model to CO_2-emission impulses is broken down to give the fractions of the impulse which reside in the atmosphere, oceans, and terrestrial biosphere – all as a perturbation to background atmospheric CO_2 concentration time-profiles that correspond to different emission scenarios. For a biospheric sink driven by the CO_2-fertilization effect, we find that the biospheric fraction reaches a maximum of roughly 30% about 50 years after the impulse, which is of the same size as the oceanic fraction at that time. The dependence of these results on emission scenario and the year of the impulse are reported.

1. Introduction

Reconstruction of the global carbon cycle for the past 200 years balances emissions of CO_2 from fossil-fuel burning and land-use changes with the accumulation of CO_2 in the atmosphere and the dissolution of CO_2 in the oceans. Reconstruction efforts, however, leave a remainder that has come to be known as the *Missing Sink*, of a significant fraction of the emitted CO_2. As the name implies, the fugitive carbon has not been accounted for although hypotheses for neglected effects have been proposed (Schimel et al., 1994). Foremost (Bazzaz and Fajer, 1992; Wigley, 1993), is the enhanced growth of the terrestrial biosphere by the increase in atmospheric CO_2 concentration, the *CO_2-Fertilization Effect*. Alternatively, Schindler and Bayley (1993) have suggested that anthropogenic fixation of nitrogen has enhanced the storage of carbon in both the marine and terrestrial biosphere and thus accounts for at least part of the missing carbon; indeed, there is evidence of anthropogenic nitrogen fixation's effect on phytoplankton growth (Owens et al., 1992). Another explanation proposed by Dai and Fung (1993) is that past variations of climate have led to a net growth of the terrestrial biosphere. Finally, regrowth of forests on previously deforested land (Dixon et al., 1994) and the buildup of soil carbon on pasture lands (Fisher et al., 1994) – not accounted for in estimates of land-use

Climatic Change **33:** 31–62, 1996.

change – are thought to account for part of the missing sink (Schimel et al., 1994). In a recent Intergovernmental Panel on Climatic Change (IPCC) report (Schimel et al., 1994) CO_2 fertilization was listed as the largest potential carbon-sink of these contributors. However, it is not our intention to advocate the hypothesis that CO_2 fertilization is the primary cause for the missing carbon-sink, but rather to study the implications of this hypothesis.

There is significant uncertainty in projecting the size of the future missing sink when the mechanism by which it operates, let alone its cause, is unknown. Nevertheless, the estimated size of the current missing sink is large enough that it is likely to be a significant contributor to the future CO_2 budget; therefore the missing sink should not be simply ignored in descriptions of future carbon cycle. So for analysis of the future CO_2-emissions scenarios – e.g., for the stabilization of greenhouse-gas concentrations – some modelers (e.g., see Enting et al., 1994) have opted to include, in global carbon-cycle models, submodels to estimate the size of the missing sink. The primary mechanism selected in model studies is the CO_2-fertilization effect. In fact, carbon-cycle models designed for analysis of emissions scenarios seem to fall into two categories: those that do not account for the missing carbon-sink and, therefore, cannot balance the past CO_2 budget, and those that account for the missing sink by assumption of the CO_2-fertilization effect along with other proposed mechanisms. Intercomparison of these models does tell us the sensitivity of model estimates to the modeling assumption of the CO_2-fertilization effect; however, intercomparison does not imply the accuracy of the estimates.

In this paper we estimate the size of the terrestrial-biospheric sink under the assumption that the past missing carbon-sink was due to the CO_2-fertilization effect. We use the carbon-cycle model contained in the Integrated Science Model (ISM) developed by Jain et al. (1994b) for use in analysis of CO_2-emission scenarios and integrated assessment models. This model has been included in the recent IPCC model intercomparison study (Enting et al., 1994; Schimel et al., 1994), and has been used to study the implications of a revised carbon budget and make projections of carbon-cycle's response to various scenarios for anthropogenic emissions of CO_2 included in the IPCC Second Assessment Report (Houghton et al., 1996). Using this model which includes the CO_2-fertilization mechanism, the size of the future terrestrial-biospheric sink is estimated. These results show the size of future carbon-sinks implied by the modeling assumption that CO_2-fertilization is the primary cause for the missing sink of carbon.

2. Model Description

The extent to which a carbon-cycle model can reliably project the future behavior of the 'real world' remains severely limited given our lack of understanding of the mechanism responsible for the missing sink. The purpose of the model we use in this study is to represent the behavior of models intended for analysis of the

anthropogenic effects on the global carbon cycle with the assumption that the CO_2 fertilization is responsible for the missing sink. An intercomparison (Enting et al., 1994) with 17 other carbon-cycle models intended for analysis of the anthropogenic effects on global carbon cycle found this carbon-cycle model response to lie well within the range of other model responses.

The globally averaged model for carbon cycle we use is depicted in Figure 1 and consists of four carbon reservoirs: the atmosphere, the terrestrial biosphere, the mixed layer of the ocean, and the deep ocean. The atmosphere and mixed layers are modeled as well mixed reservoirs. The deep ocean, however, is treated as an advective-diffusive medium with a continuous distribution of dissolved inorganic carbon described by a one-dimensional conservation of mass equation characterized by eddy diffusivity κ and upwelling velocity w (Hoffert et al., 1981). Jain et al. (1995a) determined parameter values $\kappa = 4700$ m^2/yr and $w = 3.5$ m/yr by calibration of model results to the estimated global-mean pre-anthropogenic depth-profile of ocean-^{14}C concentration. Water upwells through the deep-ocean column to the mixed layer from where it is returned, presumably through the polar sea, as bottom water to the bottom of the ocean column thereby completing the thermohaline circulation. The response of bottom-water carbon concentration to changes in mixed-layer concentration is modeled parametrically by the parameter $\pi = 0.5$ as described in detail by Jain et al. (1995a). Air–sea exchange is modeled by an air/sea exchange coefficient in combination with the buffer factor ξ that summarizes the chemical re-equilibration of sea water in response to CO_2 variations (Jain et al., 1995a). An additional carbon-source term is added to the deep-ocean model to account for the oxidation of particulate organic carbon (POC). An equivalent sink of carbon due to new production of POC in the mixed layer and the source of carbon due to particulate oxidation at intermediate depths contribute to a 5–10% lower concentration of dissolved inorganic carbon (ΣCO_2) in surface waters compared to deep waters. The buffer factor is calculated from the set of equations for borate, silicate, phosphate, and carbonate equilibrium chemistry and the temperature-dependent equilibrium constants as given by Peng et al. (1987).

To estimate terrestrial biospheric fluxes, a six-box globally-aggregated terrestrial biosphere sub-model is coupled to the atmosphere box. The six boxes represent ground vegetation, non-woody tree parts, woody tree parts, detritus, mobile soil (turn-over time 75 years), resistant soil (turnover time 500 years). The mass of carbon contained in the different reservoirs and their turnover times as well as the rate of exchange between them have been based on the analysis by Harvey (1989b) with additional references cited in that paper. The rate of photosynthesis by terrestrial biota is thought to be stimulated by increasing atmospheric carbon dioxide concentration. The increase in the rate of photosynthesis, relative to preindustrial times, is modeled to be proportional to the logarithm of the relative increase in atmospheric CO_2 concentration from its pre-industrial value of 278 ppm. The proportionality constant β, known as the CO_2-fertilization factor, is chosen to be

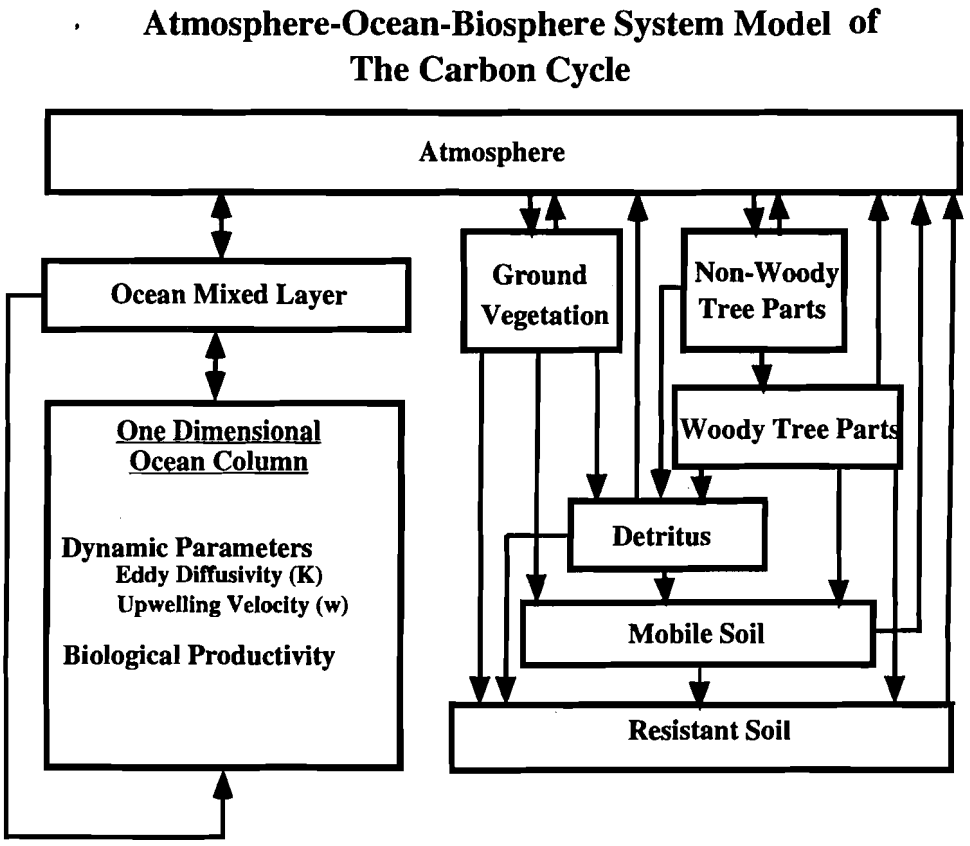

Figure 1. Schematic diagram of the global carbon-cycle model.

0.42. The rate coefficients for exchange to and from terrestrial biosphere boxes are modeled to depend on global mean temperature.

This model does contain temperature feedbacks on the carbon cycle through the prescription of the temperature-dependent buffer factor ξ, and exchange (respiration and photosynthesis) rates to and from the biosphere boxes which follow the 'Q_{10} formulation' described in the Appendix. Increases in either temperature or CO_2 lead to an increase of Net Primary Productivity (NPP) and Net Photosynthesis (NP) for the boxes for ground vegetation and non-woody tree parts, respectively. For the ground vegetation box, the equilibrium biomass is assumed to increase by the same factor as the change of NPP from changes in both CO_2 and temperature. For the non-woody tree part box, the equilibrium biomass is assumed to change by the same factor as the change of NP due to changes in CO_2 alone; this is because temperature change also leads (in this model) to a change of translocation from non-woody to woody tree parts. With this model parameterization, changing from a translocation-rate coefficient which is temperature-enhanced to one which is temperature-independent causes the temperatue effect on the terrestrial biospheric

carbon-sink to change from a sink to a source of atmospheric carbon. Furthermore, there remains significant controversy concerning the strength of the effect of temperature on respiration and net primary productivity – a succinct discussion is given by Rotmans and Den Elzen (1993). The temperature/biospheric sink feedback used in this model is, however, a gross simplication of the climate/biosphere feedbacks that have been suggested (Prentice and Fung, 1990; Dai and Fung, 1993). Furthermore, the additional effect of climate on the nitrogen cycle, which in turn affects the carbon cycle, may well be an important feedback in regions where there is nitrogen limitation of primary production (Melillo et al., 1993; Hudson et al., 1994). Moreover, nitrogen limitation of terrestrial systems is widespread in forests of the northern temperate zone, where the missing sink is thought to be located (Tans et al., 1990; Sarmiento and Sundquist, 1992; Cias et al., 1995). In interpreting the results of this model, these factors should be kept in mind.

In this model, global-mean surface temperature is estimated with an energy-balance model (Harvey and Schneider, 1985) driven by the radiative forcing change caused by CO_2 and other greenhouse gases. For the cases shown in this study, however, only the radiative forcing of CO_2 is included. Including the forcing of the other gases, and aerosols which are thought to have significant effects especially over land, would require scenarios for their emissions as well as a consideration of their connection with the emissions of CO_2 in the study of impulse responses which follows. In this study, the prescribed climate sensitivity (equilibrium temperature change for doubled CO_2 partial pressure) is $\Delta T_{2x} = 2.5$ °C. While results of this simple energy-balance model does show global warming with increased atmospheric CO_2, this model is not capable of reproducing the complicated variations of climate seen in the past records. Variations in precipitation and temperature could affect the storage of carbon in the terrestrial biosphere.

The model does include the effects of carbon emissions caused by changing land use by specification of a scenario. Land-use emissions are assumed to come from each of the terrestrial biosphere boxes in proportion to the mass of carbon in the box. Photosynthesis and respiration rates are adjusted so that the terrestrial biosphere model will not exhibit regrowth from a previously specified land use emission. The net terrestrial biosphere emission dN_b/dt is equal to the model calculated sink $S_{\text{biospheric feedbacks}}$ due to biospheric feedbacks (CO_2 fertilization and temperature effects) minus land-use emissions $E_{\text{land use}}$:

$$\frac{dN_b}{dt} = S_{\text{biospheric feedbacks}} - E_{\text{land use}} . \quad (1)$$

An alternative to specifying a land-use *emissions* scenario $E_{\text{land use}}$, is to model the emissions that result as a response to a scenario for the actual changes in land use. By doing so, Rotmans and Den Elzen (1993) were able to explicitly model the effects of changing land used on each of the biospheric carbon reservoirs. This alternative approach may prove useful for calculating, for example, the effects of forest regrowth. Implicit in our approach is that forest regrowth be accounted for in the land-use emission scenario.

The magnitude of the modeled biospheric sink is dependent on the chosen value of the CO_2-fertilization factor (Harvey, 1989a, b; Wigley, 1993; Wuebbles et al., 1995). By varying the ambient CO_2 partial pressure for individual plants in controlled experiments under ideal growing conditions, a CO_2-fertilization effect has been demonstrated and found to lead to CO_2-fertilization factors ranging from 0.2 to 0.8 (Gates, 1985; Kohlmaier et al., 1987). Nutrient limitation and community competition for resources may, however, severely diminish ecosystem response to changing atmospheric CO_2 partial pressure (Bazzaz and Fajer, 1992). The value used here of $\beta = 0.42$, however, is *not* prescribed by CO_2-fertilization experiments. The modeled magnitude of the CO_2-fertilization effect is chosen here to lead to a reconstruction of the past carbon cycle, described below, that matches the land-use emission estimate (Schimel et al., 1994) of 16 GtC (gigaton carbon GtC = 10^{12} kgC) for the decade 1980–1989. While exact parameter values (e.g. β, k and w) are used in this model, their values are derived by means of parameter estimation from the past reconstruction of the cycles of carbon and its isotopes (^{13}C and ^{14}C) and are highly uncertain based on the uncertainty of the past data records (Enting and Pearman, 1987; Kheshgi et al., 1995). Uncertainty of the estimated model parameters is one contributor to the uncertainty of future projections of atmospheric CO_2.

3. Reconstruction of the Past Carbon Cycle

The atmospheric and oceanic data that make up the past records of carbon dioxide and carbon isotopes form one basis for our understanding of anthropogenic influences on the global carbon cycle. This data is augmented by our understanding of (1) ocean transport, chemistry and biology, (2) plant physiology, ecosystem response and soil carbon, and (3) isotopic fractionation. While the reconstructions of the past records do give us information on where the sinks were (e.g., oceanic vs. biospheric) and the time history of their strengths, the reconstructions provide only circumstantial evidence as to the cause for the sinks. While detailed models of plant physiology have been developed, a 'bottom-up' approach, their extension to a global response of the terrestrial biosphere compounds uncertainty contributed at each level of detail. Whether a detailed model or a simple parametric model is used, a constraint on a carbon-cycle model is that it reproduces the past records of carbon dioxide and carbon isotopes. In this section we review the comparison of our carbon-cycle model with an assumed carbon-sink due to the CO_2-fertilization effect to past records before using this model to study the implications of this assumption to future scenarios.

The past variation of atmospheric CO_2 concentration is reproduced in the model by adjusting the magnitude of the CO_2 emissions due to changes in land use. The past variation of atmospheric CO_2 concentration and fossil-fuel emissions are well-known (Boden et al., 1991), whereas estimates of CO_2 from changes in land

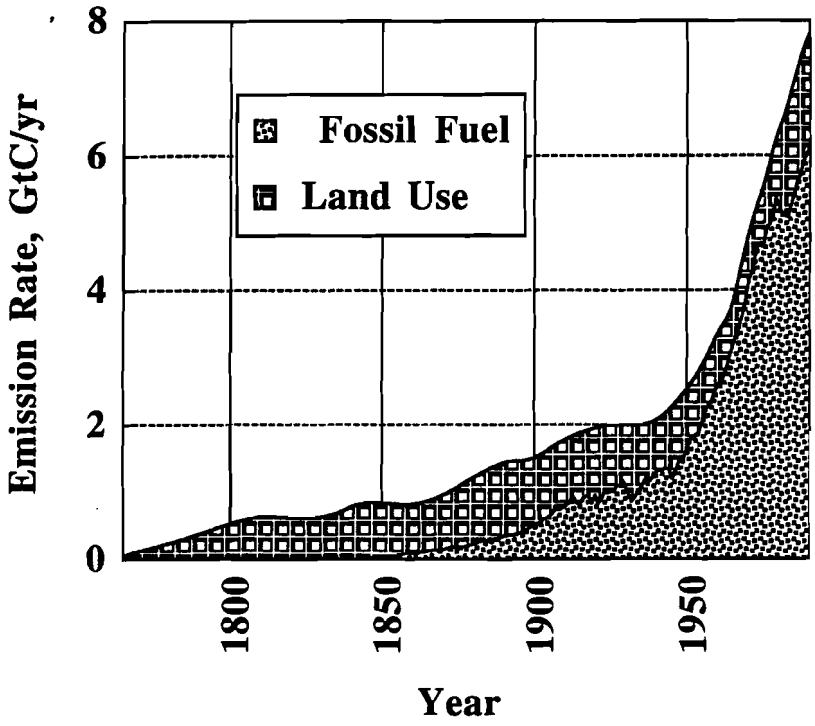

Figure 2a.

use contain great uncertainty (Schimel et al., 1994). The observed record of CO_2 concentration from 1765 to 1959 is obtained from infrared-laser spectroscopy measurements based on air taken from different layers of the Siple ice-core (Friedli et al., 1986), and thereafter it is from atmospheric measurements at the Mauna Loa Observatory in Hawaii (Keeling et al., 1989a; Keeling and Whorf, 1993). The global emission rate of CO_2 by burning of fossil fuels, $E_{\text{fossil fuel}}$, based on Boden et al. (1991) is shown in Figure 2(a). The model is used to calculate the rate of accumulation dN_o/dt of carbon in the oceans, and the rate of accumulation $S_{\text{biospheric feedback}}$ of carbon in the terrestrial biosphere (not including the effects of land-use change) by specifying the mass of carbon in the form of CO_2 in the atmosphere N_a. The model estimate of the global emission rate of CO_2 from changes in land use is determined by

$$E_{\text{land use}} = \frac{dN_a}{dt} + \frac{dN_o}{dt} + S_{\text{biospheric feedback}} - E_{\text{fossil fuel}} \cdot \tag{2}$$

The rate of land-use emissions $E_{\text{land use}}$ calculated in this way is shown in Figure 3 to be well within the error bounds (± 1GtC/yr) of estimates of land-use emissions summarized by Enting et al. (1994). The estimate of land-use change (Enting et al., 1994) shown in Figure 3(a), however, is based primarily on change of land use in tropical regions, and may not account for the effects of forest regrowth at

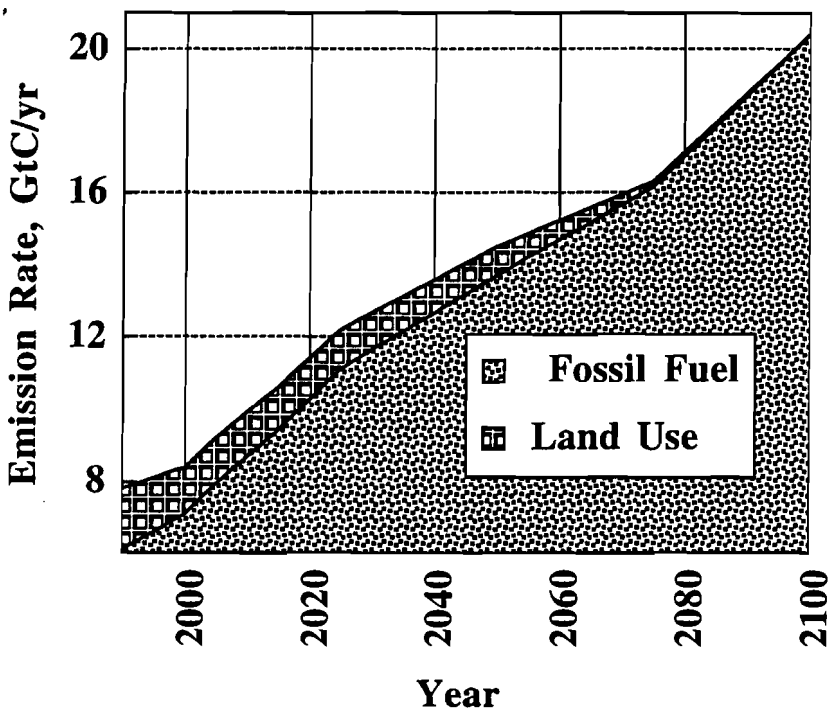

Figure 2b.

mid-latitudes. Regrowth at mid-latitudes are thought to lead to a net sink of carbon of 0.5 ± 0.5 GtC/yr for the 1980s (Schimel et al., 1994) which would modify the global land-use emissions estimate (Enting et al. 1994) to a lower value. This suggests that the value of $\beta = 0.42$ which is calibrated to give land-use emissions of 1.6 GtC/yr for the 1980s – in compliance with Enting et al.'s (1994) model intercomparison guidelines – is higher than our best estimate. Furthermore, the time-variability of $E_{\text{land use}}$ calculated from (2) – which is related to the variability in measured atmospheric CO_2 – may well be caused by sources other than the variability of land-use emissions. Analysis (Keeling et al., 1989a; Tans et al., 1993; Jain et al., 1994a) of CO_2 and ^{13}C records shows that the variability in measured atmospheric CO_2 is due in part to the variability of both the oceanic and net-biospheric sinks; such variability in these sinks is not represented in this model nor any of the carbon-cycle models designed for scenario analysis.

Variations in oceanic and biospheric sinks inferred from atmospheric CO_2 and ^{13}C records have been shown to correlate with both ENSO events and the observed (not modeled) record of global temperature (Keeling et al, 1989a). In addition, the quaternary record of atmospheric CO_2 variations also correlates with temperature, although cause and effect remain uncertain (Prentice and Fung, 1990; Saltzman and Verbitsky, 1994). However, Dai and Fung (1993) used detailed temperature

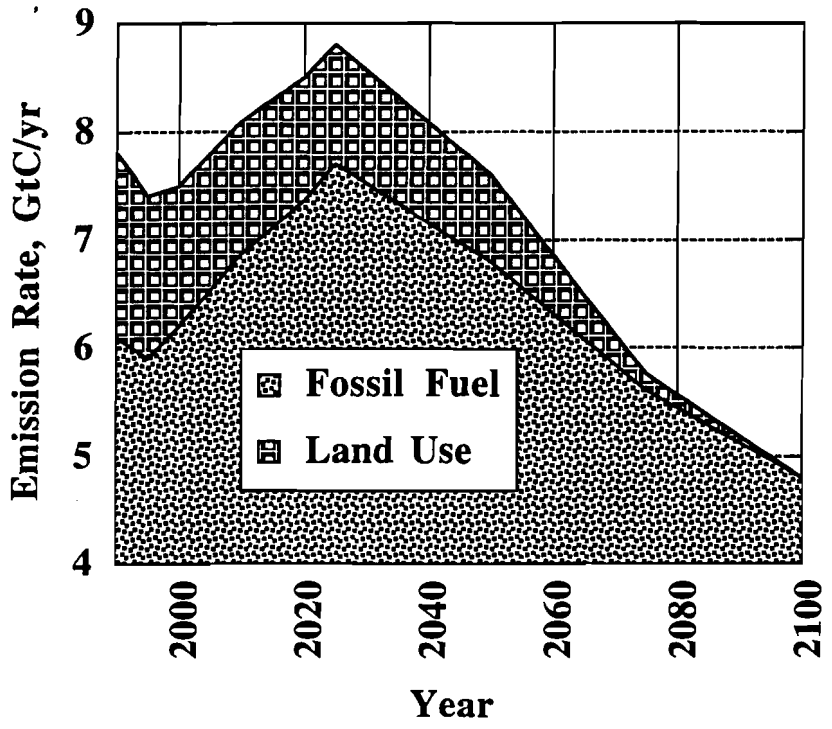

Figure 2c.

and precipitation data to show that climate changes may have caused an uptake of carbon by the terrestrial biosphere during the 1980s when there was a net global warming – the opposite sign effect than would be expected from the correlations to globally aggregated temperature. It is interesting to note that despite our poor understanding of the net effects of climate on the terrestrial-biospheric sink, Schimel et al. (1994) attributed a carbon sink of from 0 to 1 GtC/yr to this feedback during the 1980s. In our model, the choice of Q_{10} parameters leads to the result that increase in global temperature results in a small sink of carbon, similar to the IPCC estimate (Schimel et al., 1994). In our view, however, the uncertainty in the climate/biospheric feedback is so great that our modeled feedback should be viewed as only illustrative. These apparent effects can explain some of the discrepancy between the model-inferred and observation-based estimates of land-use emissions shown in Figure 3.

This schematic model for the carbon cycle is constructed to be consistent with current understanding of the global carbon cycle. Validation of the capability of the model to represent this understanding is partially based on the analysis of tracer records such as those for ^{13}C and ^{14}C; therefore, in addition to reproducing the past record of CO_2 concentration it is important that a carbon-cycle model also be able to reproduce tracer records. Different tracers are sensitive to different components

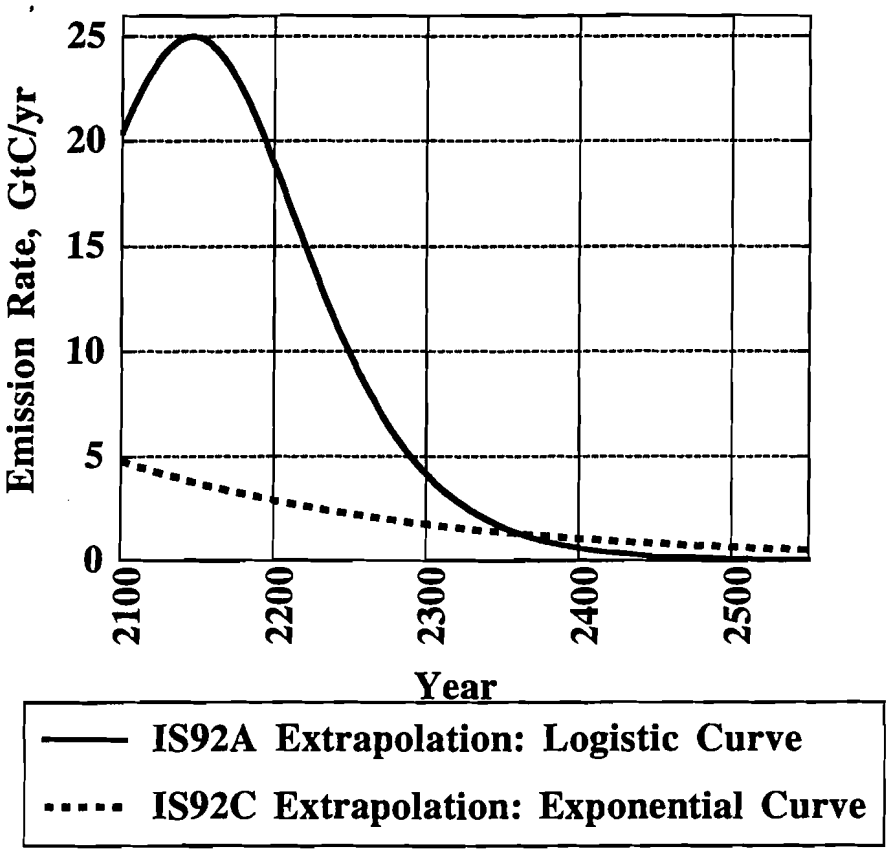

Figure 2d.

Figure 2. Emissions of CO_2 from the burning of fossil fuels and changes in land use. (a) Past record of land-use emissions (calculated from the atmospheric record using an inverse model), and fossil-fuel emissions. (b) IPCC (Leggett et al., 1992) emissions scenario IS92a. (c) IPCC (Leggett et al., 1992) emissions scenario IS92c. (d) Extrapolation of IPCC emission scenarios beyond 2100.

of the model. For example, the modeled absorption of CO_2 by the oceans is closely related to the ocean inventory of bomb-produced ^{14}C from atmospheric nuclear testing in the 1950s and early 1960s (Siegenthaler and Joos, 1992). The past variation of ^{13}C is related to the emission or uptake of CO_2 by the terrestrial biosphere and fossil-fuel burning, because of the significant isotopic fractionation of terrestrial–biospheric and fossil-fuel carbon which occurs during photosynthesis. Earlier studies (Jain et al., 1994a, 1995a, b) have demonstrated that the model is able to reproduce the depth-dependence of ^{14}C and dissolved inorganic carbon in the oceans, the dilution of ^{14}C by fossil-fuel emissions (the Suess Effect), the ocean inventory of bomb-produced ^{14}C, and variations of past atmospheric CO_2, ^{13}C and bomb-^{14}C.

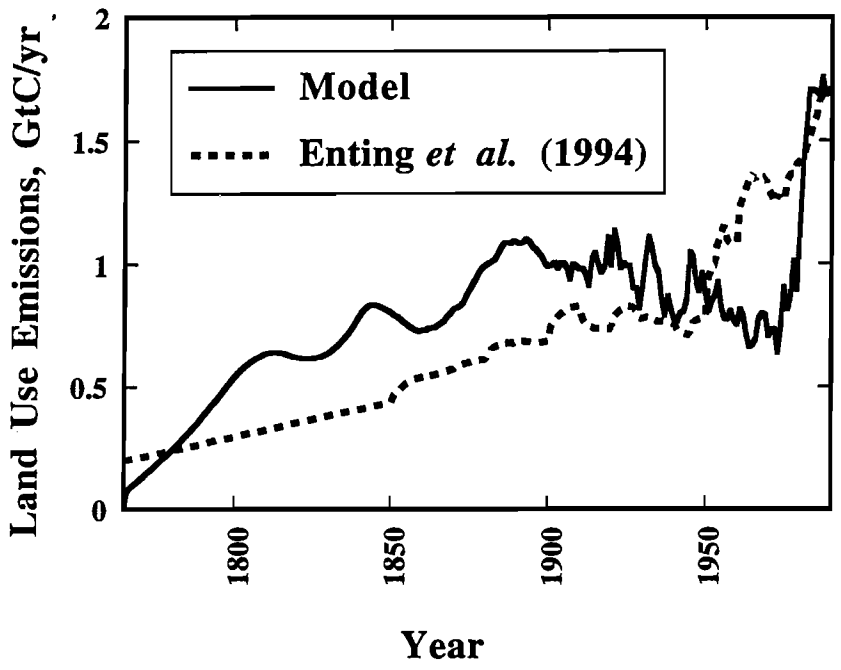

Figure 3. Comparison of land-use emissions calculated from equation (2) by model reconstruction of past carbon cycle (solid line) is compared to the IPCC (Enting et al., 1994; Schimel et al., 1994) estimates of emissions from changes in land use (dashed line).

For the period 1765–1989 and 1980–1989 Table I lists the net changes and emissions reconstructed using this model. These results for 1980–1989 are nearly identical to those determined by Rotmans and Den Elzen (1993), given in their Table 4, as well as those listed by Schimel et al. (1994). The magnitude of the biospheric feedback is sizable, compensating for land-use emissions over the decade 1980–1989 to give a net terrestrial–biospheric accumulation of close to zero (+0.9 GtC in our analysis). The atmosphere accumulates the greatest fraction of emitted carbon over these time scales, followed by the oceans.

Tracer responses could determine future carbon-cycle response *if* (i) the carbon-cycle system were linear, and (ii) there were not other poorly understood drivers of the carbon cycle. In our model, we include several important nonlinearities in which we have varying degrees of confidence. The ocean buffer factor is well determined by independent measurements of ocean chemistry (Peng et al., 1987). And the logarithmic dependence of direct radiative forcing on CO_2 concentration is a firm conclusion of studies of radiative heat transfer. If these were the only nonlinearities present in the system (and there were no unknown or unprecedented drivers) then the response of the carbon-cycle system could be well characterized by past responses (Kheshgi and White, 1995). Other nonlinearities that are included are the logarithmic dependence of CO_2 fertilization on CO_2 concentration, and

Table I
Model reconstruction of the past carbon budget for the period from 1765 to 1989

	1765 to 1989	1980 to 1989	1980 to 1989	
			IPCC 1994 (Schimel et al., 1994)[f]	Rotmans and Den Elzen (1993)[h]
Fossil-fuel emissions[a]	212.8 Gt C	54.4 Gt C	55 ± 5 Gt C	54 Gt C
Atmospheric accumulation[b]	159.4 Gt C	33.2 Gt C	32 ± 2 Gt C	34 Gt C
Modeled ocean accumulation	124.2 Gt C	20.3 Gt C	20 ± 8 Gt C	21.5 Gt C
Net biospheric accumulation[c]	−70.8 Gt C	+0.9 Gt C		−1.5 Gt C[i]
Modeled Bio-spheric feedback[e]	105.3 Gt C	16.9 Gt C		
Land-use emissions[d]	176.1 Gt C	16.0 Gt C[e]	11 ± 11 Gt C[g]	

[a] Fossil fuel taken from Boden et al. (1991).
[b] Atmospheric accumulation is calculated from the changes in atmospheric CO_2 concentration measured from the Siple ice core (Friedli et al., 1986) and at the Mauna Loa Observatory (Keeling et al., 1989a; Keeling and Whorf, 1993) over the time periods listed in the Table.
[c] Net biospheric accumulation calculated by subtraction.
[d] Land-use emissions calculated by subtraction.
[e] The magnitude of the modeled biospheric feedback is adjusted by choice of β to result in 16. Gt C land-use emissions for the time period 1980–1989.
[f] The uncertainty is meant to represent a 90% confidence interval.
[g] This value is the sum of the estimate of the carbon source due to changes in tropical land use (16 ± 10 Gt C), and the carbon sink due to Northern Hemisphere forest regrowth (5 ± 5 Gt C).
[h] The case given by Rotmans and Den Elzen (1993) with feedbacks to balance the carbon budget is shown.
[i] Rotmans and Den Elzen (1993) have labeled this value as emissions from land-use change, while with our nomenclature this is the net biospheric accumulation.

the Q_{10} formulation of the response of the terrestrial biosphere rate coefficients on global temperature. While there is some empirical evidence to support the nonlinearities used in the terrestrial-biospheric model (Harvey, 1989a), there are alternative formulations which would give different responses when conditions change enough to make the nonlinear effects evident. For example, instead of a logarithmic dependence of CO_2-fertilization on CO_2 concentration, some studies (Wigley, 1993; Sarmiento et al., 1995) have opted to use a Michaelis–Menten formulation which exhibits an absolute saturation (with increasing CO_2 concentration)

of rates of carbon fixation at a prescribed level. While the near term response of the two different CO_2-fertilization formulations are similar, their responses would depart at high CO_2 concentration. Other potential drivers of carbon cycle could be future changes in precipitation or nitrogen cycle (Galloway et al., 1995), and prediction of either is currently problematic. For these reasons the tracer records *alone* are insufficient to determine the future response of the carbon cycle.

These tracer records, nevertheless, provide important guidance in determining the past size of the oceanic and terrestrial–biospheric sinks; these records tell where the sink lies, but do not indicate the mechanisms by which these sinks operate. Projections of future atmospheric CO_2 levels depend on the mechanisms for these sinks assumed in a carbon-cycle model. Being able to reproduce past tracer records does not explicitly prove the accuracy of a model to project future values. However, reproduction of past tracer records is a requirement for carbon-cycle model analysis; such validation does constrain the range of possible model results.

4. Carbon-Cycle Response for Scenarios of Future Emissions

Estimates of future CO_2 concentration depend on the scenario for CO_2 emissions as well as the size of the ocean and biosphere sinks. Two scenarios for future CO_2 emissions are considered in this study. Figure 2b and 2c show the emissions from 1990 to 2100 for CO_2 corresponding to Scenarios IS92a and IS92c of the IPCC (Leggett et al., 1992). Scenario IS92a is a close approximation to the earlier IPCC (Houghton et al., 1990) Business as Usual Scenario. In scenario IS92a, CO_2 produced from fossil-fuel burning and cement production increases by factor of three from 1990 to 2100. For the low emissions IPCC scenario IS92c, CO_2 produced from fossil-fuels and cement production show a 23% reduction from 1990 to 2100. Both scenarios share the same emissions from land-use change. CO_2 emissions from forest burning are considerably reduced by 2100. In the late 21st century there is a small rate of CO_2 absorption from the atmosphere due to reforestation that brings the net emissions from land-use change to zero by 2100.

For the two IPCC scenarios the carbon-cycle model, with CO_2 fertilization accounting for the missing sink, is used to estimate the amount of carbon that is transferred to the oceans and terrestrial biosphere. Over the period from 1990 to 2100, the atmospheric concentration of CO_2 increases, as shown in Figure 4. This causes the magnitude of the ocean and biospheric-feedback sinks to both increase, as can be seen by comparing Tables I and II. The reason for the increase of the ocean sink is that the atmospheric partial pressure of CO_2 continues to increase relative to the deep-ocean partial pressure of CO_2; since the ocean sink is limited by mixing between water below and above the thermocline (for time periods on the order of a century), the magnitude of the ocean sink is related to the difference in partial pressures adjusted for the effects of the biological pumping (which is

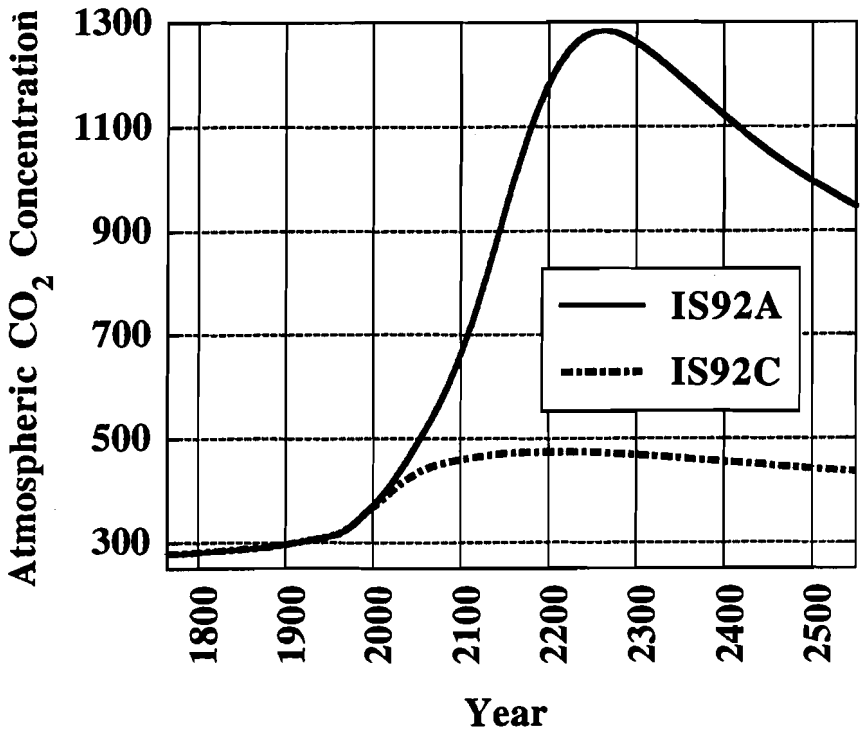

Figure 4. Model calculated atmospheric CO_2 concentration as a response to the record of past emissions (with land-use emissions calibrated to match the atmospheric record of CO_2 concentration) and scenarios for future emissions.

assumed to be unchanging in time) of carbon by particulate settling (Volk and Liu, 1988) through the thermocline. The reason for the increase in the biospheric feedback sink is the logarithmic dependence of the net primary productivity (NPP) on the partial pressure of CO_2 (pCO_2):

$$\frac{\mathrm{d}(NPP)}{\mathrm{d}(p\mathrm{CO}_2)} = \beta \times \frac{NPP_{1765}}{p\mathrm{CO}_2} . \tag{3}$$

The temperature-enhanced productivity (NP and NPP) of plants is a weaker effect, in the model, than the CO_2-fertilization effect and adds to the biospheric feedback sink. The temperature-enhanced respiration (see Appendix) is yet a smaller effect that leads to a small decrease in the biospheric sink. What is noticeable in Tables I and II is that previous to the 1980s the net biospheric accumulation of carbon was negative, whereas following the 1980s it is positive. This is due to emissions from land-use change being overwhelmed by the increasing CO_2-fertilization effect; this is in large part due to the model assumptions that the land-use emissions will decrease from the 1980s (contained in the scenario), and that the missing sink is accounted for, primarily, by the CO_2-fertilization effect which is assumed to follow (3).

Table II

The net changes and emissions reconstructed using this model for the period from 1990 to 2100

	1990 to 2100		1990 to 1999	
	IS92a	IS92c	IS92c	IS92c
Fossil-fuel emissions scenario	1446.2 Gt C	705.3 Gt C	65.5 Gt C	59.3 Gt C
Land-use emissions scenario	83.4 Gt C	83.4 Gt C	15.3 Gt C	15.3 Gt C
Modeled atmospheric accumulation	656.6 Gt C	226.5 Gt C	33.7 Gt C	28.9 Gt C
Modeled ocean accumulation	501.4 Gt C	334.4 Gt C	26.1 Gt C	25.0 Gt C
Modeled biospheric feedback	371.6 Gt C	227.8 Gt C	21.0 Gt C	20.7 Gt C
Net biospheric accumulation	288.2	144.4 Gt C	5.7 Gt C	5.4 Gt C

To examine the long term (≈500 yr) response of the carbon-cycle model to impulses of carbon to the atmosphere requires long-term scenarios for carbon emissions. These scenarios are extrapolations of the two IPCC scenarios which end at 2100 and are not meant to be predictions. After the year 2100 we assume that there are no emissions from land-use change. Emissions from the burning of fossil-fuels are extrapolated by functions that match the emissions rate and its time rate of change at the year 2100.

For the emissions scenario IS92a, which is increasing at 2100, we extrapolate with a logistic function – similar to that used by Siegenthaler and Oeschger (1978) – given by

$$E_{\text{fossil}}(t) = \frac{\mathrm{d}}{\mathrm{d}t}\left\{\frac{5{,}000\ \text{GtC}}{1 + 2.5 \times e^{0.02\text{yr}^{-1}\times(2100-t)}}\right\} \text{ for } t > 2100\,. \tag{4}$$

This scenario eventually leads to 5,000 gigatons of carbon emissions. The intent of the scenario, as with those of Siegenthaler and Oeschger (1978) and Sundquist (1986, 1990), is to represent a case where emissions exhaust roughly the world's supply of recoverable fossil fuels.

For the emissions scenario IS92c, which is decreasing at 2100, we extrapolate with an exponential function given by

$$E_{\text{fossil}}(t) = 4.8\frac{\text{GtC}}{\text{yr}} \times e^{0.005\text{yr}^{-1}\times(2100-t)} \text{ for } t > 2100\,. \tag{5}$$

While this scenario has lower emissions in the 22nd century than the IS92a extrapolation, the IS92c extrapolation exceeds the IS92a extrapolation in the late 24th

century as can be seen in Figure 2d. The more rapid decrease of the IS92a extrapolation is intended to be due to the depletion of fossil-fuel reserves, whereas in the IS92c scenario extrapolation cumulative emissions do not reach that extent.

The carbon-cycle model is used to estimate the atmospheric CO_2 response to these scenarios of fossil fuel and land use emissions; results are shown in Figure 3. The high CO_2 levels (over 1,200 ppm) reached in the IS92a extrapolation scenario leads to *significant nonlinear effects*: high values of buffer factor (greater than 30) and some saturation of the CO_2-fertilization effect due to the logarithmic dependence of (3). These effects are evident in the system responses described next.

5. Impulse Response for Scenarios of Future Emissions

When an impulse of CO_2 is added to the atmosphere, fractions of the CO_2 will leave the atmosphere to be incorporated in the terrestrial biosphere and the oceans. The remaining CO_2 in the atmosphere is known as the airborne fraction. We study the model response of a small impulse of carbon to the background of each of the emissions scenarios which are large-amplitude perturbations to the carbon-cycle system and definitely outside of the linear regime. If the size of the impulse is small enough, however, then the modeled response of the mass of carbon in the atmosphere, oceans and terrestrial biosphere can be approximated as a *linear* function of the impulse mass δ. In this limit the response of the carbon reservoirs to an impulse at time $t_{\text{perturbed}}$ is

$$N_{a,\,\text{perturbed}}(t) = N_a(t) + \delta \times f_a(t, t_{\text{perturbed}}) \,, \tag{6a}$$

$$N_{o,\,\text{perturbed}}(t) = N_o(t) + \delta \times f_o(t, t_{\text{perturbed}}) \,, \tag{6b}$$

$$N_{b,\,\text{perturbed}}(t) = N_b(t) + \delta \times f_b(t, t_{\text{perturbed}}) \,, \tag{6c}$$

where, N_a, N_o, and N_b are the mass of carbon in the atmosphere, oceans, and terrestrial biosphere (including soils). In the results that follow we use an impulse size of $\delta = 1$ GtC; we have used the model to test the accuracy of using a finite size pulse and have concluded that this contributes an error, compared to the small impulse limit, in airborne fraction f_a of no greater than 0.0001 for results shown.

The impulse response is useful in calculating the effect that an incremental change in CO_2 emissions will have over the time after the impulse. Impulse–response functions have been used in past studies to define global warming potentials for greenhouse gases. While some gases, such as CFC's, decay exponentially with time with a clearly defined half-life, CO_2 does not. Summaries of carbon-cycle results, as was given by e.g., Moore and Bradswell (1994), in terms of atmospheric half-life must, therefore, be interpreted with care. The airborne fraction of CO_2 is dependent on the atmospheric CO_2 concentration, and therefore on the scenario

for CO_2 emissions. Of course, the airborne fraction will also depend on the size of the modeled ocean and terrestrial–biospheric sinks. In the following we consider several cases.

The primary dependence of the atmospheric, ocean and biospheric fractions, f_a, f_o, and f_b is on the time after impulse $t - t_{\text{perturbed}}$: see Figure 5. Initially the atmospheric fraction is one. Over the first couple of years the ocean fraction grows faster than does the biospheric fraction, with the atmospheric fraction decreasing accordingly. Over the next few decades the biospheric fraction grows more rapidly than the ocean fraction to the point at which they both are of similar size. Over the following centuries the biospheric fraction decreases in size because of the saturation of the CO_2-fertilization effect with the higher background CO_2 concentration estimated for the future for the two emissions scenarios considered. (The biospheric fraction could decrease even more with time if a Michaelis–Menten formulation of the CO_2-fertilization effect were chosen with a low NPP-saturation level.) While ocean CO_2 solubility also becomes more saturated because of the increase of the buffer factor for higher future CO_2 concentrations, the ocean fraction continues to increase due to continued transport of carbon down to the deep ocean.

As can be seen in Figure 5 the atmospheric, ocean and biospheric fractions depend on both the time of the impulse and the scenario for CO_2 emissions. The largest ocean and biospheric fractions develop at low CO_2 conditions, as in the 1930 pulse for the IS92c scenario. And the smallest ocean and biospheric fractions develop at high CO_2 conditions, as in the 2050 pulse for the IS92a scenario. This is because the modeled capacity of the oceans and the biosphere to take up carbon decreases, the greater the level of atmospheric CO_2. In the oceans this is caused by a buffer factor that increases with increasing pCO_2. In the biosphere this is caused by a Net Primary Productivity that increases with pCO_2 less rapidly at higher levels of pCO_2 than at lower levels of pCO_2; and this is, of course, a consequence of the hypothesis that the missing carbon-sink is due to CO_2-fertilization.

The nonlinear dependence of the modeled ocean and biospheric carbon-sinks on pCO_2 are remarkably similar to each other. This can be seen by comparing the ratio of biospheric to ocean fraction of the impulses at different times and for different emission scenarios, as shown in Figure 6. At high background pCO_2 conditions, the response of the ratio of fractions seems to approach an asymptote – for example, compare the 1990 and 2050 impulses for scenario IS92a. And so the strength of the modeled nonlinear dependence on pCO_2 is quite similar for both the ocean and the biospheric sinks. Also evident in Figures 5 and 6 is that the ocean CO_2 sink responds initially faster than does the biospheric sink. This is because the mixing of CO_2 into the ocean-surface waters is a faster process than the increased rate of photosynthesis at short times after the impulse. After about a decade, the biospheric fraction has reached roughly the same size as the ocean fraction. If the CO_2-fertilization effect is used to account for the missing carbon-sink, then the size of the biospheric sink is as large as the ocean sink. This is in contrast with many

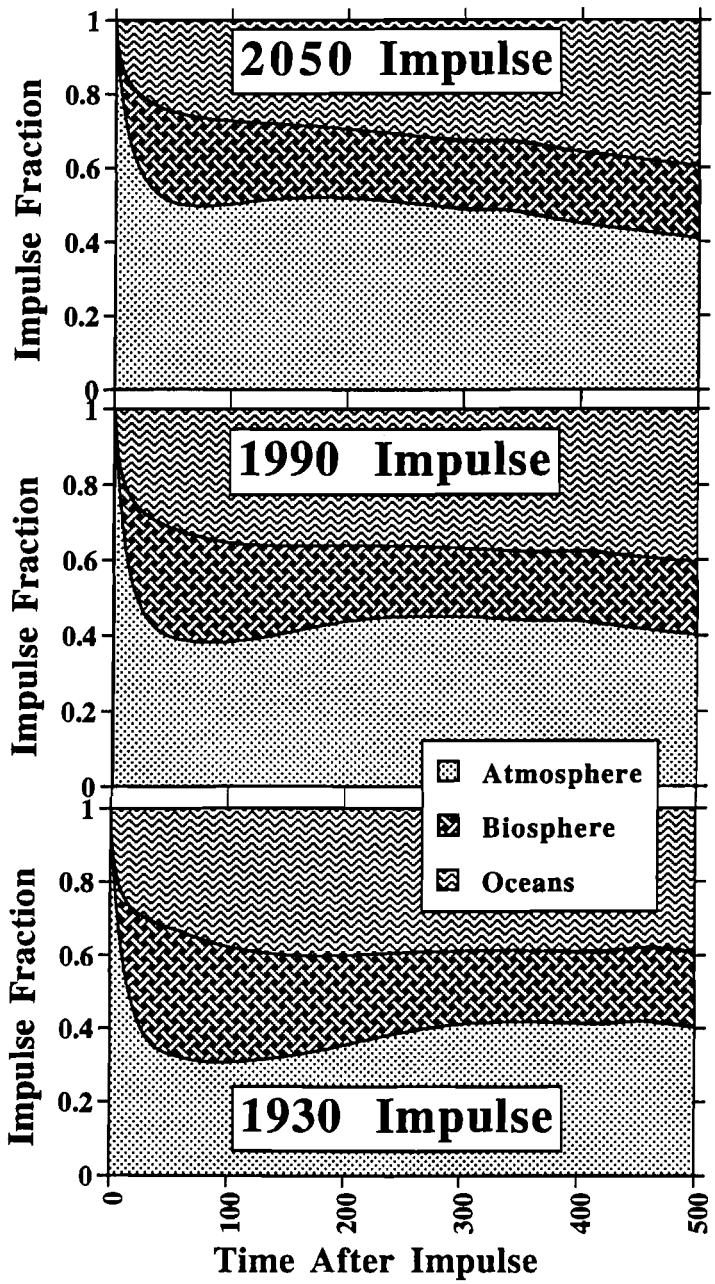

Figure 5a.

descriptions of the carbon cycle that state that the oceans are the primary sink of carbon.

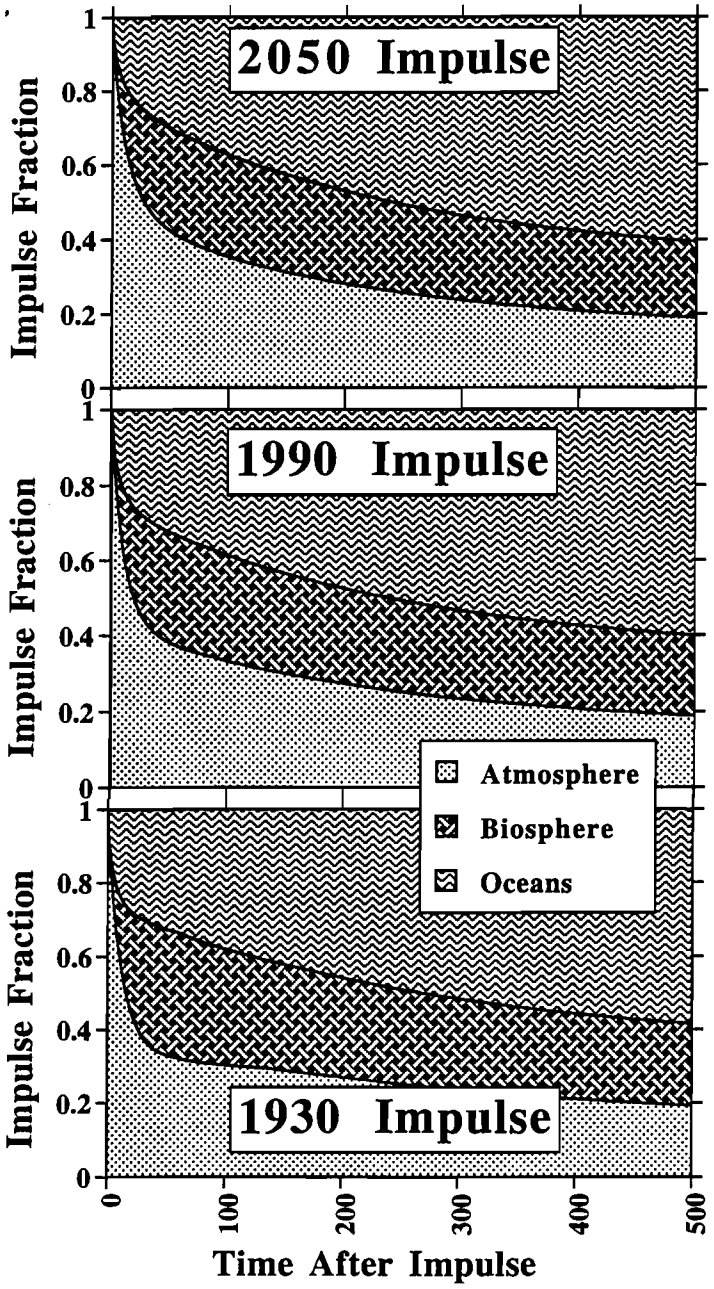

Figure 5b.

Figure 5. Model calculated response to a small (one Gt carbon) impulse of CO_2 to the atmosphere. Fraction of the impulse that resides in the atmosphere, terrestrial biosphere, and oceans are estimated for impulses emitted to the atmosphere at three different times: 1930, 1990 and 2050. The background CO_2 level, shown in Fig. 4, changes in response to the past record and future scenarios for CO_2 emissions. Two scenarios for future emissions are considered: (a) the IPCC (Leggett et al., 1992) emissions scenario IS92a with a logistic function extrapolation beyond the year 2100, and (b) the IPCC (Leggett et al., 1992) emissions scenario IS92c with an exponential function extrapolation beyond the year 2100.

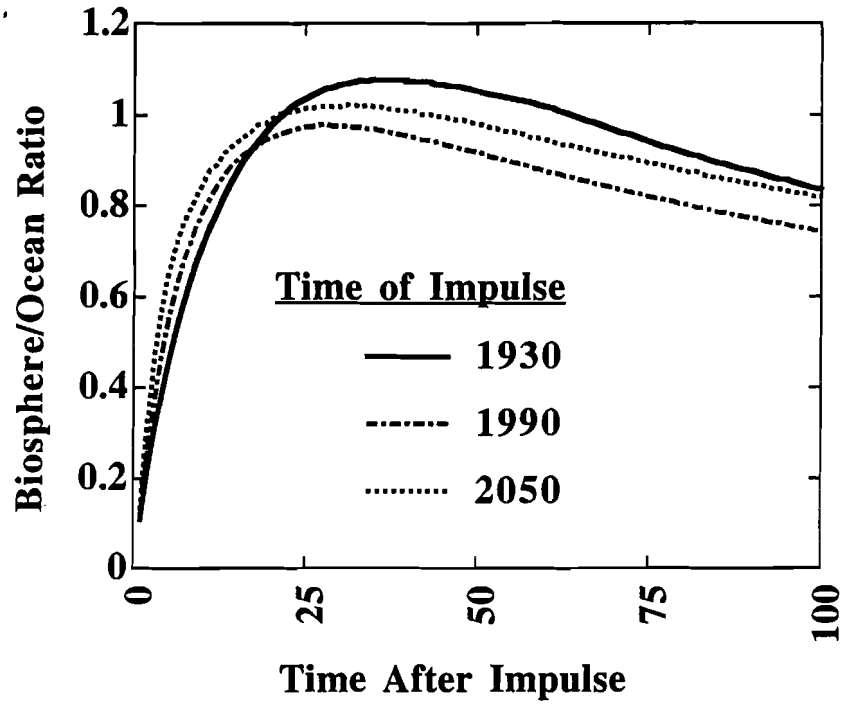

Figure 6a.

It is clear from the cases depicted in Figure 5 that there is not a single atmospheric lifetime for carbon emitted to the atmosphere. In some cases, over some periods of time after impulse, the airborne fraction of carbon even increases with time – see, for example, impulse responses shown in Figure 5a for times 200 years after impulse. Again, this is because of the nonlinear effects included for both the ocean and biospheric sinks. Including the biospheric sink both decreases the airborne fraction and increases the extent to which the airborne fraction will increase with time due to higher background CO_2 levels.

Different amounts of the carbon taken up by the biosphere goes into the different carbon reservoirs depicted as the six boxes in Figure 1. For the impulse responses, Tables III and IV list the fraction of carbon that goes into each box at times 20, 100 and 500 years after the impulse. Up to 100 years, more than half of the carbon uptake by the biosphere resides in the woody parts of trees. The turnover time of the woody-tree reservoir is constrained by estimates of Net Primary Productivity of forests and forest biomass (Schlesinger, 1991), supporting our assumed model turnover time. Initially there is an increase in soil-carbon fraction followed by a reduction in the soil fraction caused by both temperature-enhanced respiration and saturation of the CO_2-fertilization effect. Nevertheless, the soil fraction continues to increase *relative* to the woody biomass. In the IS92a case the soil fraction becomes as large as the woody fraction after 500 years. In the IS92c case the soil

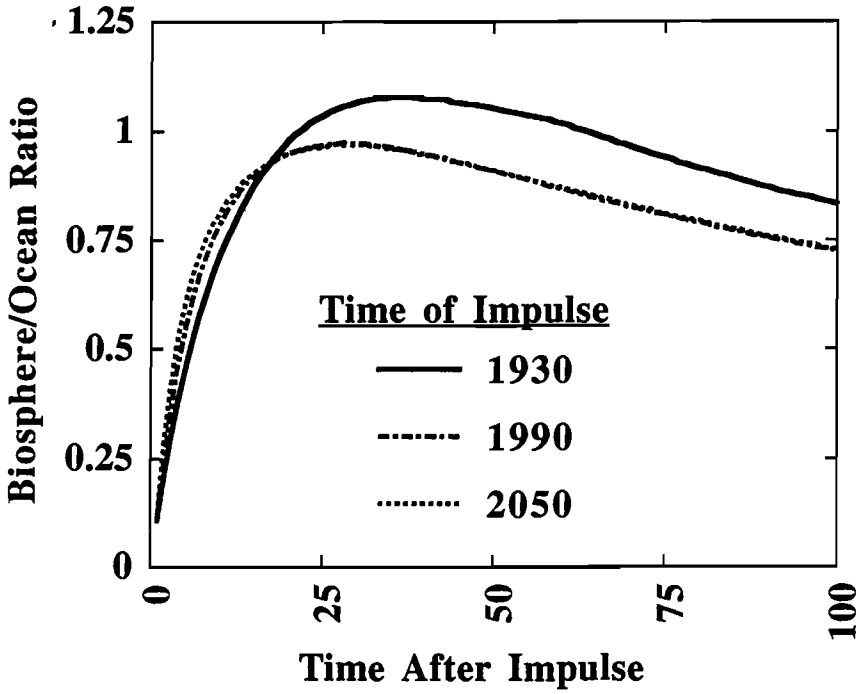

Figure 6b.

Figure 6. The ratio of the fraction of an atmospheric CO_2 impulse that resides in the terrestrial biosphere to the fraction that resides in the oceans is estimated with the global carbon-cycle model shown in Fig. 1. Estimates given for impulses emitted to the atmosphere at three different times: 1930, 1990 and 2050. Biosphere/ocean ratio reaches a maximum about 30 years after the impulse. The background CO_2 level, shown in Fig. 4, changes in response to the past record and future scenarios for CO_2 emissions. Two scenarios for future emissions are considered: (a) the IPCC (Leggett et al., 1992) emissions scenario IS92a with a logistic function extrapolation beyond the year 2100, and (b) the IPCC (Leggett et al., 1992) emissions scenario IS92c with an exponential function extrapolation beyond the year 2100. The biospheric fraction is of comparable size to the ocean fraction, except at short time periods (less than ten years) after the impulse.

fraction becomes larger than the woody fraction 500 years after the impulse. Of course there can be many other effects that could impact soil-carbon over such long time-scales, especially if these soils are under cultivation.

In the modeled cases the biosphere fraction accounts for a maximum of roughly 30% of the impulse. This reaches a maximum about 50 years after the impulse, and rises to near the maximum after about ten years. This time scale is important if these results are to be used in integrated assessment models (at least the current conceptualization of them) because many of these models weight the benefits of reduced CO_2 levels more heavily in the near future than in the distant future by use, for example, of a discount rate. For example, Nordhaus (1992) uses an annual discount rate of 4% which will weight the airborne fraction over the first

Table III

Atmospheric, oceanic and biospheric fractions of a small CO_2 impulse to the atmosphere for the emissions scenario IS92a

$t-t_{perturbed} \Rightarrow$	20 years			100 years			500 years		
$t_{perturbed} \Rightarrow$	1930	1990	2050	1930	1990	2050	1930	1990	2050
Atmosphere	0.452	0.495	0.603	0.308	0.383	0.503	0.405	0.401	0.409
Oceans	0.277	0.259	0.2	0.377	0.354	0.274	0.39	0.405	0.396
Terrestrial biosphere	0.271	0.246	0.198	0.315	0.263	0.224	0.204	0.194	0.196
Ground vegetation	0.021	0.015	0.009	0.008	0.005	0.003	0.003	0.002	0.002
Non-woody tree parts	0.013	0.011	0.008	0.006	0.005	0.004	0.003	0.003	0.003
Woody tree parts	0.165	0.161	0.139	0.154	0.139	0.13	0.095	0.094	0.097
Detritus	0.025	0.021	0.015	0.012	0.009	0.007	0.005	0.005	0.005
Mobile soil	0.041	0.034	0.024	0.104	0.08	0.061	0.04	0.038	0.039
Resistant soil	0.005	0.005	0.003	0.031	0.024	0.019	0.058	0.051	0.048

Table IV

Atmospheric, oceanic and biospheric fractions of a small CO_2 impulse to the atmosphere for the emissions scenario IS92c

$t-t_{perturbed} \Rightarrow$	20 years			100 years			500 years		
$t_{perturbed} \Rightarrow$	1930	1990	2050	1930	1990	2050	1930	1990	2050
Atmosphere	0.452	0.493	0.554	0.302	0.331	0.352	0.192	0.189	0.188
Oceans	0.277	0.26	0.229	0.381	0.388	0.375	0.584	0.601	0.606
Terrestrial biosphere	0.271	0.247	0.217	0.317	0.281	0.273	0.224	0.21	0.205
Ground vegetation	0.021	0.015	0.012	0.008	0.007	0.007	0.004	0.004	0.004
Non-woody tree parts	0.013	0.011	0.009	0.006	0.005	0.005	0.003	0.003	0.003
Woody tree parts	0.165	0.161	0.148	0.155	0.146	0.148	0.086	0.083	0.081
Detritus	0.025	0.021	0.017	0.013	0.011	0.011	0.007	0.006	0.006
Mobile soil	0.041	0.034	0.027	0.104	0.086	0.079	0.056	0.053	0.052
Resistant soil	0.005	0.005	0.004	0.031	0.025	0.022	0.067	0.061	0.059

several decades more heavily than the remaining time. A very similar approach has been used by Haraden (1993) in estimating the shadow cost of CO_2 emissions. The biospheric fraction does increase rapidly enough, and is strong enough to affect estimates of the economic impact of CO_2 emissions generated by integrated assessment models. These findings are a result of several model assumptions: (i) CO_2-fertilization is the primary cause for the missing sink which is budgeted 16 GtC for the 1980s; (ii) the nonlinear dependence of the CO_2-fertilization effect follows (3); and (iii) the turnover times for the biosphere carbon reservoirs. There is some support for these assumptions, especially over time scales of decades. The carbon budget is constrained by CO_2 and isotopic records. We do not expect the near term (several decades) response to be highly dependent on the form of nonlinearity (3). And the turnover time for plants, which are expected to respond

first, is constrained by observations. The primary assumption that remains is that CO_2-fertilization is responsible for the missing sink.

6. Alternative Causes for the Terrestrial Biosphere Carbon-sink

Other mechanisms for the terrestrial biosphere carbon-sink will lead to differing magnitudes of biospheric feedback to CO_2 emission. The implications of the uncertainty in the nature of the feedback is explored by comparing the impulse responses of the carbon-cycle model to a CO_2 impulse when two different models are assumed for the biospheric feedback: (i) the CO_2-fertilization/temperature-dependent-rate model described in the Appendix, and (ii) a model with no biospheric feedback. The impulse responses are compared in Figure 7 for a 1990-impulse perturbation to emission scenario IS92a. In both cases the unperturbed biospheric sink is taken to be equal to that of the CO_2-fertilization/temperature-dependent-rate model so that the unperturbed atmospheric concentration and the past carbon cycle (and tracer) reconstruction are identical for both model assumptions. Of course, when there is no biospheric feedback, then there is no biospheric fraction of impulse carbon. The thick curve in Figure 7 divides the airborne fraction of the impulse (below the curve) from the oceanic fraction (above the curve). The thick curve shows that the carbon that would go to the biosphere with the CO_2-fertilization/temperature-dependent-rate model is partitioned (in the model without biospheric feedback) between the atmosphere and oceans to maintain an atmosphere/ocean fraction ratio (as a function of time after impulse) that is nearly the same for the two model assumptions. Both models show a decrease in airborne fraction for roughly the first 100 years after the impulse, followed by an increase caused by the saturation of ocean and biospheric sinks with rising background CO_2, followed by a decrease corresponding to decreasing CO_2-background concentration as seen in Figure 4.

The effects of CO_2-fertilization and temperature-dependent rate coefficients in the biosphere model (see Appendix) are shown separately in Figure 8 for a 1990-impulse to the IS92a emission scenario (as in Figure 7). Three curves are shown that represent the effects of combinations of the biospheric feedbacks: (i) both the CO_2-fertilization and temperature-dependent rate-coefficient feedbacks, (ii) the CO_2-fertilization feedback alone, and (iii) the temperature-dependent-rate-coefficient feedback alone. The temperature-dependent rate-coefficient feedback contributes a net carbon-sink for the biosphere that is smaller than that contributed by the CO_2-fertilization effect; this is consistent with estimates (Schimel et al., 1994) of the magnitude of the CO_2-fertilization feedback (0.5–2.0 GtC/yr for the 1980s) and the climate/biospheric feedback (0–1 GtC/yr for the 1980s). While both processes contribute to the total biospheric fraction, their fractions are not exactly additive. The CO_2-fertilization effect accounts for the decrease in impulse fraction following the maximum in biospheric fraction; this is due, in the model, to the logarithmic dependence of the CO_2-fertilization effect on the partial pressure of

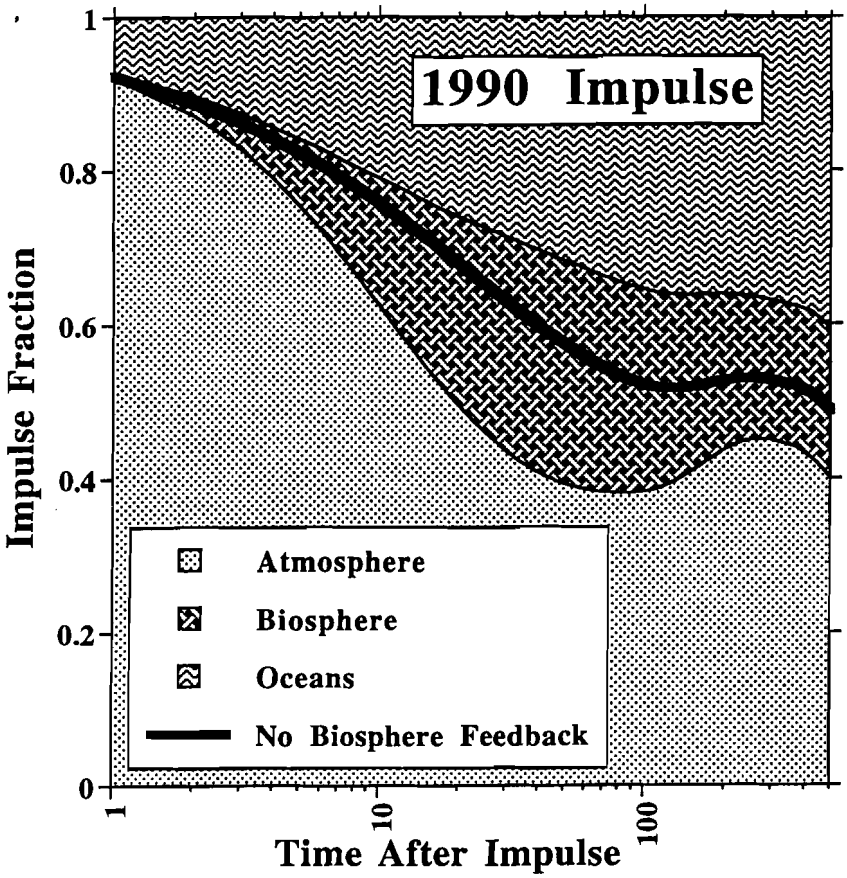

Figure 7. Model calculated response to a small (one Gton carbon) impulse of CO_2 to the atmosphere. The background CO_2 level, shown in Figure 4, changes in response to the past record and the future scenarios for CO_2 emissions which follows the IPCC (Leggett et al., 1992) emissions scenario IS92a with a logistic function extrapolation beyond the year 2100. The fraction of the impulse that resides in the atmosphere, terrestrial biosphere, and oceans are shown for an impulse emitted to the atmosphere in 1990 for two different model assumptions. First, where the biospheric feedback is given by the CO_2-fertilization/temperature-dependent-rate model; this model result is shown by the patterns in this figure, and is identical to that shown in the Figure 5a center panel except that it is plotted with a logarithmic time scale. And second, where the missing sink is modeled by some process in which terrestrial carbon storage is not affected by the concentration of CO_2 so that the biospheric fraction is zero (no biospheric feedback); this model result is shown by the thick curve which indicates the split between the atmospheric fraction (below the curve) and the oceanic fraction (above the curve).

CO_2. The temperature feedback also shows a similar time evolution due to the logarithmic dependence of radiative forcing on CO_2 concentration; the maximum and minimum, however, occur at greater times after the impulse due to the thermal inertia of the modeled ocean which causes the background temperature to lag changes in CO_2 concentration.

Forest regrowth (Dixon et al., 1994) or soil buildup (Fisher et al., 1994) that happens as a response to human-induced changes in land use or vegetation, and

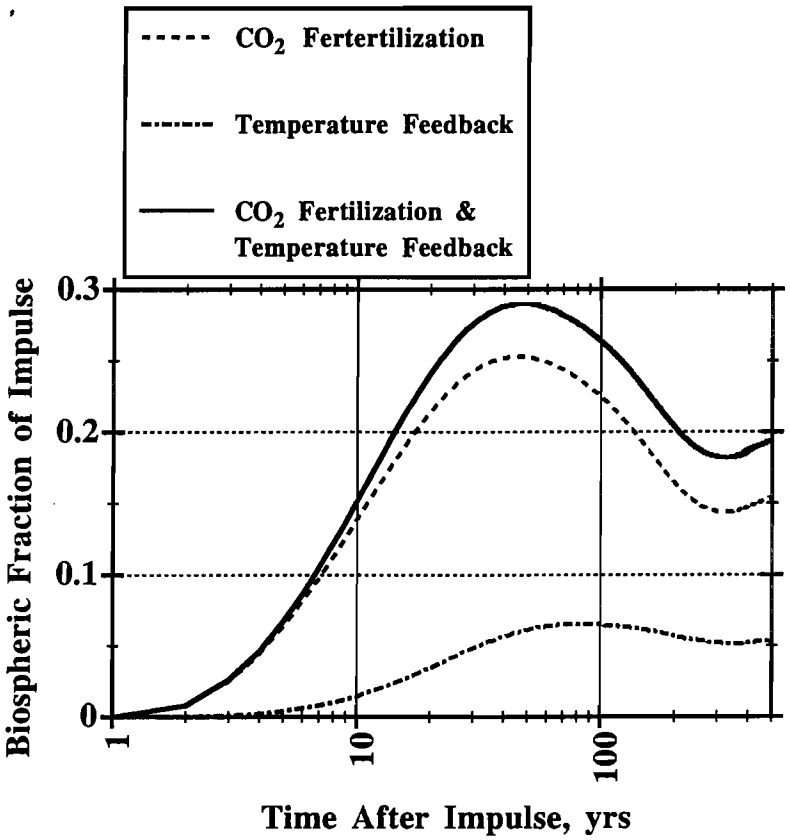

Figure 8. Model calculated response to a small (one Gton carbon) impulse of CO_2 to the atmosphere. The background CO_2 level, shown in Fig. 4, changes in response to the past record and the future scenarios for CO_2 emissions which follows the IPCC (Leggett et al., 1992) emissions scenario IS92a with a logistic function extrapolation beyond the year 2100. The fraction of the impulse that resides in the terrestrial biosphere is shown for an impulse emitted to the atmosphere in 1990 for three different model assumptions for the biospheric feedback. First, where the biospheric feedback is modeled by the CO_2-fertilization effect alone. Second, where the biospheric feedback is modeled by temperature-dependent biospheric rate coefficients alone. And third, where the biospheric feedback is modeled by both the CO_2-fertilization effect and temperature-dependent biospheric rate coefficients (this is the same size biospheric fraction as is shown in Fig. 5a).

are not compensated for in estimates of net CO_2 emissions attributed from land-use change (Schimel et al., 1994), would probably not have a great sensitivity to atmospheric CO_2 concentration although land-management practices would likely have a strong effect. In this case, the biospheric feedback to atmospheric CO_2 would probably be negligible as in the alternative model whose impulse response is shown in Figure 7.

The fertilization of the biosphere by anthropogenic emissions of nitrogen-containing compounds is not directly related to atmospheric CO_2 concentration, and so is not expected to have a strong biospheric feedback to CO_2 emissions;

however, emissions of NO_x, for example, are produced by many of the same activities that emit CO_2 and would, therefore, indirectly lead to a biospheric feedback. The changes in climate that are estimated to result from CO_2 emissions could have effects on the biosphere not accounted for in the model used in this report. For example, an additional feedback mechanism is the incorporation of soil nitrogen released as a result of climate change by plants which have a higher C/N ratio than the soil, and this would lead to a net biospheric sink of carbon; the interactions between climate change, and nitrogen and CO_2 fertilization and the resulting effects on carbon cycle have been modeled by more complex models for the terrestrial biosphere (Hudson et al., 1994).

The difference between the results of the two model assumptions shown in Figure 7 does imply the magnitude of one component of our uncertainty in estimating carbon-cycles response to emissions of greenhouse gases. Similarly, studies which have looked in detail at the sensitivity of model results to model parameters such as β (Harvey, 1989a, b; Wigley, 1993; Wuebbles et al., 1995) do characterize one component of uncertainty, but not all the uncertainties. Clearly there are variations in the CO_2 record, both seasonal and interannual (Keeling et al., 1989a), that are of a magnitude greater than the uncertainty that can be explained by this model intercomparison. We do not suggest that this type of comparison alone be used to quantify the magnitude of our uncertainty in estimates of the future carbon cycle.

Implicit in this model for the carbon cycle and the use of the impulse responses to illustrate model behavior is the premise that the rate of carbon uptake by the oceans and terrestrial biosphere is determined by the history of the atmospheric concentration of CO_2. For the oceans, one basis for this is the relation between the solubility of CO_2 and the atmospheric concentration of CO_2. For the terrestrial biosphere, the model representation of the CO_2 fertilization effect, likewise, is consistent with this premise. There are, however, observed correlations between the inferred uptake of CO_2 and phenomena such as ENSO events or interannual changes in climate (Keeling et al., 1989a) that imply that carbon uptake is driven by the chaotic behavior of these phenomena over short time-scales. Over century time-scales, large shifts in the carbon cycle have not been detected over the last millennium prior to the industrial revolution, suggesting that the observed interannual variability may be limited to short time-scales and small magnitude. Nevertheless, there remains a fundamental question as to the predictability of the climate/carbon-cycle system perturbed by the anthropogenic emissions of CO_2, and other human-induced effects.

7. Concluding Discussion

Detailed analysis of the carbon budget reveals the need for a carbon-sink in addition to that expected by the oceans (Siegenthaler and Oeschger, 1987). Completion of the ^{13}C budget gives a strong indication that this sink lies within the terrestrial

biosphere (Broecker and Peng, 1993; Cias et al., 1995). While several mechanisms have been proposed for the enhanced growth of the terrestrial biosphere in recent years (Dai and Fung, 1993; Rotmans and Elzen, 1993; Schindler and Bayley, 1993; Dixon et al., 1994), foremost is the CO_2-fertilization effect. While the cause of the missing sink remains a mystery, we consider the implications of the hypothesis that the missing sink is due to the CO_2-fertilization effect.

Past trends in atmospheric CO_2, ^{13}C and ^{14}C are consistent with a carbon-cycle model including the CO_2-fertilization effect. Our model, which consists of a one-dimensional ocean model with recirculation of polar bottom water and a six-box terrestrial biosphere model, is sufficient to reproduce atmospheric trends. Variations on a time-scale of several years, however, are not predicted by our globally aggregated model. An example of such a short time-scale fluctuation was the cessation of atmospheric CO_2 rise from 1990 to 1993. Analysis of ^{13}C concentration in conjunction with globally aggregated models can be used to investigate which carbon reservoir is responsible for the fluctuation (Keeling et al., 1989b; Jain et al., 1994a). The mechanisms responsible for these short time-scale fluctuations remain unknown, preventing prediction. Even though the mechanism for the long-term trend in the missing sink also remains unknown, the past trend can be modeled. How well our model extrapolations can project future concentrations depends in large part on how well our model for the CO_2-fertilization effect mimics the true cause of the missing carbon-sink.

We consider two scenarios for CO_2 emissions from land-use change and the burning of fossil fuels: the IPCC scenarios IS92a and IS92c (Leggett et al., 1992). Over the time period from 1990 to 2100 we find that the response of the biosphere accounts for the uptake of 24% and 29% of emissions for the two scenarios respectively (from Table II). We also interrogate our model carbon cycle by examining its response to impulses of CO_2 to the atmosphere. We find that the fraction of CO_2 taken up by the biosphere increases with time until it reaches a maximum of roughly 30% about 50 years after the impulse. The biospheric fraction at this time is as large as the modeled oceanic fraction. These results, of course, depend on the scenario and time of the impulse, as shown above. Nevertheless, the assumption that the missing carbon-sink is caused by the CO_2-fertilization effect, according to our model mechanism, leads to the conclusion that at least 20% (from Tables III and IV) of CO_2 emissions will be sequestered by the terrestrial biosphere.

Our conclusions are also based on the assumption that the intrinsic behavior of the global terrestrial carbon cycle follows that of the past. Significant changes in land use will likely alter the types of existing plants which could have a different response to changing atmospheric composition and climate. This could cause, for example, a change in the globally aggregated CO_2-fertilization coefficient with time, and there may have already been a significant shift due to past land use changes. The rapid increase in the application of fertilizer may have global effects (Galloway et al., 1995). A nonlinear response of the biosphere may cause it to behave unlike it has in the past. Warming climate may lead to massive forest

dieback releasing carbon, or wetter climate may lead to soil-carbon preservation. Unless these effects have been experienced in the past, confirmation of these potential effects would have to occur without the guidance of the past records of global atmospheric CO_2 or carbon isotopes making the case for each effect much harder to prove. In this study, the assumption of a CO_2-fertilization effect with a logarithmic dependence on CO_2 concentration shows the terrestrial biosphere to be a significant future sink of carbon.

Appendix

The terrestrial fluxes are estimated by a globally aggregated, six-box terrestrial biosphere sub-model. The six boxes shown in Figure 1 represent carbon reservoirs for: (i) ground vegetation (59 GtC), (ii) non-woody tree parts (38 GtC), (iii) woody tree parts (634 GtC), (iv) detritus (96 GtC), (v) mobile soil (700 GtC), and (vi) resistant soil (800 GtC) where the initial mass (steady-state value at 1765) of the respective box is given in brackets. The first two reservoirs fix carbon by photosynthesis while all six reservoirs release carbon by respiration. The flow of carbon between reservoirs is due to the physical movement of fixed carbon from one reservoir to another. One of the soil boxes is a rapid turnover box (mobile soil box) with turnover time of 70 years and the other soil box is a slow turnover box (resistant soil box) with turnover time of 500 years.

The equations describing mass balance in two photosynthetic boxes, are of the form

$$\frac{\mathrm{d}B_i}{\mathrm{d}t} = \left(v_i - \sum \alpha_{ij}\right) B_i - \rho_i B_i^2 - Flu_i \qquad \text{for } i = 1, 2. \tag{A1}$$

The governing equations for other boxes are of the form

$$\frac{\mathrm{d}B_i}{\mathrm{d}d} = \left(-\alpha_{ia} - \sum \alpha_{ij}\right) B_i + \sum \alpha_{ji} B_j - Flu_i \qquad \text{for } i = 3, \ldots, 6 \tag{A2}$$

where i is the number of the biospheric boxes listed above, B_i is the mass of box i, α_{ij}, and α_{ji} are the exchange coefficients for carbon fluxes from box i to box j and vice versa, α_{ia} is exchange coefficient for the carbon flux from box i to atmosphere, v_i and ρ_i are the parameters controlling net primary productivity (NPP for the ground vegetation box) or net photosynthesis (NP for the non-woody tree parts box), and Flu_i is the net land use flux from box i to the atmosphere. The initial values of v and ρ for ground vegetation are 0.504 yr^{-1} and 0.004 GtC^{-1} yr^{-1} and for non-woody tree parts they are 1.672 yr^{-1} and 0.002 GtC^{-1} yr^{-1}. The initial exchange coefficients between the terrestrial boxes and the atmosphere as well as between different terrestrial components are taken from Emanuel et al. (1984). Their values are:

$\alpha_{ia} = 0.022,\ 0.531,\ 0.013,$ and $0.002\ yr^{-1}$ for i = 3–6

$\alpha_{1j} = 0.169,\ 0.078,$ and $0.0062\ \text{yr}^{-1}$ for $j = 4,\ 5$ and 6

$\alpha_{2j} = 0.816$ and $0.794\ \text{yr}^{-1}$ for $j = 3$ and 4

$\alpha_{3j} = 0.022,\ 0.0044,$ and $0.00034\ \text{yr}^{-1}$ for $j = 4,\ 5$ and 6

$\alpha_{4j} = 0.029$ and $0.0023\ \text{yr}^{-1}$ for $j = 5$ and 6

$\alpha_{5j} = 0.0011\ \text{yr}^{-1}$ for $j = 6$

The rate coefficients are temperature-dependent according to

$$M = M_0(Q_{10})^{(T-T_0)/10\,^\circ\text{C}} \tag{A3}$$

where M_0 is the initial rate of coefficient M, T_0 is the initial temperature, and Q_{10} is the factor by which a given reaction increases for a temperature increase of 10 °C. For the small relative changes in absolute temperature being considered, the Q_{10} formulation is virtually the same as an Arrhenius formulation of the temperature dependence of rate coefficients. A Q_{10} of 1.4 is used for the NPP of ground vegetation and of 1.53 is used for the NP of non-woody tree parts; the rates of NPP and NP are represented by the term $v_iB_i - \rho_iB_i^2$ in (A.1) for $i = 1$ and 2, respectively. A Q_{10} of 2.0 is used for respiration ($j = 3, \ldots, 6$) as well as the transfer of carbon from non-woody tree parts to woody tree parts. The separate Q_{10}'s for NP and respiration give a tree-NPP with an effective Q_{10} of about 1.4. The Q_{10}'s for the transfer of carbon from plants to soils is zero, while the transfer of carbon between soil boxes ($j = 4,\ 5,\ 6$) is 2.0. The justification for these feedbacks can be found in Harvey (1989a), Marowitch et al. (1986), Reuss and Innis (1977), and Carlyle and Than (1988).

The model includes the stimulation of NP or NPP, caused by enhanced atmospheric CO_2 using the β-factor introduced by Bacastow and Keeling (1973),

$$N = N_0[1 + \beta\ \ln(\text{CO}_2(t)/\text{CO}_2(t_0))] \tag{A4}$$

where N_0 and $\text{CO}_2(t_0)$ are the initial NP or NPP and CO_2 concentration, respectively. The value of β has been described in the text.

The fluxes from the atmosphere to ground vegetation and non-woody tree parts represent NPP and NP, respectively which are modeled by a logistic law:

$$F_{ai} = v_iB_i - \rho_iB_i^2 \tag{A5}$$

where i = ground vegetation and non-woody tree parts boxes, and F_{ai} is the flux from the atmosphere to box i of size B_i.

All other fluxes are assumed to be linearly proportional to the mass of the donor box:

$$F_{ij} = \alpha_{ij}B_i$$

where F_{ij} and α_{ij} are the carbon flux and the exchange coefficient for carbon flux from box i to box j, and B_i is the mass of the donor box.

Acknowledgments

This work was supported in part by the U.S. Department of Energy through the office of Health and Environmental Research, and the Environmental Research Division.

References

Bacastow, R. and Keeling, C. D.: 1973, 'Atmospheric Carbon Dioxide and Radiocarbon on the Natural Carbon Cycle', in Woodwell, G. M. and Pecan, E. V. (eds.), *Carbon and the Biosphere*, U.S. Atomic Energy Commission, pp. 86–135.

Bazzaz, F. A. and Fajer, E. D.: 1992, 'Plant Life in a CO_2-Rich World', *Sci. Am.* **264**, 68–74.

Boden, T. A., Sepanski, R. J., and Stoss, F. W.: 1991, 'Trends 91: A Compendium of Data on Global Change', Oak Ridge Natl. Lab, Oak Ridge, USA, ORNL/CDIAC-46.

Broecker, W. S. and Peng, T. H.: 1993, 'Evaluation of the ^{13}C Constraint on the Uptake of Fossil Fuel CO_2 by the Ocean', *Global Biogeochem. Cycles* **7**, 619–626.

Carlyle, J. C. and Than, U. B.: 1988, 'Abiotic Controls of Soil Respiration Beneath an Eighteen-Year-Old Pinus Radiate Stand in South-Eastern Australia', *J. Ecol.* **76**, 654–662.

Cias, P., Tans, P. P., Trolier, M., White, J. W. C., and Francey, R.'J.: 1995, 'A Large Northern Hemisphere Terrestrial CO_2 Sink Indicated by the $^{13}C/^{12}C$ ratio of atmospheric CO_2', *Science* **269**, 1098–1102.

Dai, A. and Fung, I. Y.: 1993, 'Can Climate Variability Contribute to the "Missing" CO_2 Sink?', *Global Biogeochem. Cycles* **7**, 599–609.

Dixon, R. K., Brown, S. A., Houghton, R. A., Solomon, A. M., Trexler, M. C., and Wisniewski, J.: 1994, 'Carbon Pools and Flux of Global Forest Ecosystems', *Science* **263**, 185–190.

Emanuel, W. R., Killough, G. G., Post, W. M., and Shugart, H. H.: 1984, 'Modeling Terrestrial Ecosystems in the Global Carbon Cycle with Shifts in Carbon Storage Capacity by Land-Use Change', *Ecology* **65**, 970–983.

Enting, I. G. and Pearman, G. I.: 1987, 'Description of a One-Dimensional Carbon Cycle Model Calibrated by the Techniques of Constrained Inversion', *Tellus* **39B**, 459–476.

Enting, I. G., Wigley, T. M. L., and Heimann, M. (eds.): 1994, *Future Emissions and Concentrations of Carbon Dioxide: Key Ocean/Atmosphere/Land Analyses*, CSIRO Division of Atmospheric Research Technical Paper No. 31, CSIRO, Australia, 120 pp.

Fisher, M. J., Rao, I. M., Ayarza, M. A., Lascano, C. E., Sanz, J. I., Thomas, R. J., and Vera, R. R.: 1994, 'Carbon Storage by Introduced Deep-Rooted Grasses in the South American Savannas', *Nature* **371**, 236–238.

Friedli, H., Lotscher, H., Oeschger, H., Siegenthaler, U., and Stauffer, B.: 1986, 'Ice Core Record of the $^{13}C/^{12}C$ Ratio of Atmospheric Carbon Dioxide in the Past Two Centuries', *Nature* **324** , 237–238.

Galloway, J. N., Schlesinger, W. H., Levy II, H., Michaels, A., and Schnoor, J. L.: 1995, 'Nitrogen Fixation: Anthropogenic Enhancement-Environmental Response', *Global Biogeochem. Cycles* **9**, 235–252.

Gates, D. M.: 1985, 'Global Biospheric Response to Increasing Atmospheric Carbon Dioxide Concentration', in Strain, B. R. and Cure, J. D. (eds.), *Direct Effects of Increasing Carbon Dioxide on Vegetation*, U.S. Dept. Energy, DOE/ER-0238, Washington DC, pp. 171–184.

Haraden, J.: 1993, 'An Updated Shadow Price for CO_2', *Energy – Int. J.* **18**, 303–307.

Harvey, L. D. D.: 1989a, 'Effect of Model Structure on the Response of Terrestrial Biosphere Models to CO_2 and Temperature Increases', *Global Biogeochem. Cycles* **3**, 137–153.

Harvey, L. D. D.: 1989b, 'Managing Atmospheric CO_2', *Climatic Change* **15**, 343–381.

Harvey, L. D. D. and Schneider, S. H.: 1985, 'Transient Climate Response to External Forcing on 10^0–10^4 Year Time Scales, Part I. Experiments with Globally Averaged Coupled Atmosphere and Ocean Energy Balance Models', *J. Geophys. Res.* **90**, 2191–2205.

Hoffert, M. I., Callegari, A. J., and Hseih, C.-T.: 1981, 'A Box-Diffusion Carbon Cycle Model with Upwelling, Polar Bottom Water Formation and a Marine Biosphere', in Bolin, B. (ed.), *Carbon Cycle Modeling, SCOPE 16*, Wiley, New York, pp. 287–305.

Houghton, J. T. et al. (eds.): 1996, *The IPCC Second Scientific Assessment Report*, Cambridge University Press, Cambridge.

Houghton, J. T., Jenkins, G. J., and Ephraums, J. J. (eds.): 1990, *Climate Change, The IPCC Scientific Assessment*, Cambridge University Press, Cambridge.

Hudson, R. J. M., Gherini, S. A., and Goldstein, R. A.: 1994, 'Modeling the Global Carbon Cycle: Nitrogen Fertilization of the Terrestrial Biosphere and the "Missing" CO_2 Sink', *Global Biogeochem. Cycles* **8**, 307–333.

Jain, A. K., Kheshgi, H. S., Caldeira, K., Hoffert, M. I., and Wuebbles, D. J.: 1994a, 'Evaluation of $\delta^{13}C$ of Atmospheric Carbon Dioxide with a Schematic Carbon Cycle Model', *Amer. Geophys. Union Fall Meeting, EOS Suppl.* **75**, 152–153.

Jain, A. K., Kheshgi, H. S., and Wuebbles, D. J.: 1994b, 'Integrated Science Model for Assessment of Climate Change', Lawrence Livermore National Laboratory, UCRL-JC-116526.

Jain, A. K., Kheshgi, H. S., Hoffert, M. I., and Wuebbles, D. J.: 1995a, 'Distribution of Radiocarbon as a Test of Global Carbon Cycle Models', *Global Biogeochem. Cycles* **9**, 153–166.

Jain, A. K., Wuebbles, D. J., and Kheshgi, H. S.: 1995b, 'Can We Balance the Atmospheric Budget of Bomb-Produced Radiocarbon?', *EOS Suppl* **76**, S77.

Keeling, C. D. and Whorf, T.: 1993, 'Trends in Atmospheric CO_2 Since the Eruption of Pinatubo in 1991', in *4th Int. CO_2 Conf.*, World Meteorological Organization, Carquiranne, pp. 67–68.

Keeling, C. D., Bacastow, R. B., Carter, A. F., Piper, S. C., Whorf, T. P., Heimann, M., Mook, W. G., and Roeloffzen, H.: 1989a, 'A Three-Dimensional Model of Atmospheric CO_2 Transport Based on Observed Winds, 1. Analysis of Observational Data', in Peterson, D. H. (ed.), *Aspects of Climate Variability in the Pacific and Western Americas*, Am. Geophys. Union, Washington, DC, pp. 165–236.

Keeling, C. D., Piper, S. C., and Heimann, M.: 1989b, 'A Three-Dimensional Model of Atmospheric CO_2 Transport Based on Observed Winds, 4. Mean Annual Gradients and Interannual Variations', in Peterson, D. H. (ed.), *Aspects of Climate Variability in the Pacific and Western Americas*, Am. Geophys. Union, Washington, DC, pp. 305–363.

Kheshgi, H. S. and White, B. S.: 1995 'Modelling Ocean Carbon Cycle with a Nonlinear Convolution Model', *Tellus*, in press.

Kheshgi, H. S., Jain, A. K., and Wuebbles, D. J.: 1995, 'Uncertainty in the Global Carbon Budget Derived from Isotopic Constraints', *Am. Geophys. Union Fall Meeting, EOS Suppl.* **76**, F83.

Kohlmaier, G. H., Brohl, H., Sire, E. O., Plochal, M., and Revelle, R.: 1987, 'Modelling Stimulation of Plants and Ecosystem Response to Present levels of Excess Atmospheric CO_2', *Tellus* **39B**, 155–170.

Leggett, J., Pepper, W. J., and Swart, R. J.: 1992, 'Emission Scenarios for the IPCC: An Update', in Houghton, J. T., Callander, B. A., and Varney, S. K. (eds.), *Climate Change 1992: The Supplementary Report to the IPCC Scientific Assessment*, Cambridge University Press, New York, pp. 69–96.

Marowitch, J., Richter, C., and Hoddinott, J.: 1986, 'The Influence of Plant Temperature on Photosynthesis and Translocation Rates in Bean and Soybean', *Can. J. Bot.* **64**, 2337–2342.

Melillo, J. M., McGuire, A. D., Kicklighter, D. W., Moore III, B., Vorosmarty, C. J., and Schloss, A. L.: 1993, 'Global Climatic Change and Terrestrial Net Primary Production', *Nature* **363**, 234–240.

Moore, B. and Bradswell, B. H.: 1994, 'The Lifetime of Excess Atmospheric Carbon Dioxide', *Global Biogeochem. Cycles* **8**, 23–38.

Nordhaus, W. D.: 1992, 'An Optimal Transition Path for Controlling Greenhouse Gases', *Science* **258**, p. 1315.

Owens, N. J. P., Galloway, J. N., and Duce, R. A.: 1992, 'Episodic Atmospheric Nitrogen Deposition to Oligotrophic Oceans', *Nature* **357**, 397–399.

Peng, T.-H., Takahashi, T., Broecker, W. S., and Olafsson, J.: 1987, 'Seasonal Variability of Carbon Dioxide, Nutrients and Oxygen in the Northern North Atlantic Surface Water', *Tellus* **39B**, 439–458.

Prentice, K. C. and Fung, I. Y.: 1990, 'The Sensitivity of Terrestrial Carbon Storage to Climate Change', *Nature* **346**, 48–51.

Reuss, J. O. and Innis, G. S.: 1977, 'A Grassland Nitrogen Flow Simulation Model', *Ecology* **58**, 379–388.

Rotmans, J. and Den Elzen, M. G. J.: 1993, 'Modelling Feedback Mechanisms in the Carbon Cycle: Balancing the Carbon Budget', *Tellus* **45B**, 301–320.

Saltzman, B. and Verbitsky, M.: 1994, 'CO_2 and Glacial Cycles', *Nature* **367**, 419.

Sarmiento, J. L. and Sundquist, E. T.: 1992, 'Revised Budget of the Oceanic Uptake of Anthropogenic Carbon Dioxide', *Nature* **356**, 589–593.

Sarmiento, J. L., Le Quéré, C., and Pacala, S. W.: 1995, 'Limiting Future Atmospheric Carbon Dioxide', *Global Biogeochem. Cycles* **9**, 121–137.

Schimel, D., Enting, I., Heimann, M., Wigley, T., Raynaud, D., Alves, D., and Siegenthaler, U.: 1994, 'CO_2 and the Carbon Cycle', in Houghton, J. T. et al. (eds.), *Climate Change 1994: Radiative Forcing of Climate Change and an Evaluation of the IPCC IS92 Emission Scenarios*, Cambridge University Press, New York, pp. 35–71.

Schindler, D. W. and Bayley, S. E.: 1993, 'The Biosphere as an Increasing Sink for Atmospheric Carbon: Estimates from Increasing Nitrogen Deposition', *Global Biogeochem. Cycles* **7**, 717–733.

Schlesinger, W.: 1991, *Biogeochemistry: An Analysis of Global Change*, Academic Press, San Diego, 443 pp.

Siegenthaler, U. and Joos, F.: 1992, 'Use of a Simple Model for Studying Oceanic Tracer Distributions and the Global Carbon Cycle', *Tellus* **44B**, 186–207.

Siegenthaler, U. and Oeschger, H.: 1978, 'Predicting Future Atmospheric Carbon Dioxide Levels', *Science* **199**, 388–395.

Siegenthaler, U. and Oeschger, H.: 1987, 'Biospheric CO_2 Emissions During the Past 200 Years Reconstructed by Deconvolution of Ice Core Data', *Tellus* **39B**, 140–154.

Sundquist, E. T.: 1986, 'Geologic Analogs: Their Value and Limitations in Carbon Dioxide Research', in Trabalka, J. R. and Reichle, D. E. (eds.), *The Changing Carbon Cycle*, Springer-Verlag, New York, pp. 371–402.

Sundquist, E. T.: 1990, 'Influence of Deep-Sea Benthic Processes on Atmospheric CO_2', *Phil. Trans. Roy. Soc. A* **331**, 155–165.

Tans, P. P., Berry, J. A., and Keeling, R. F.: 1993, 'Oceanic $^{13}C/^{12}C$ Observations: A New Window on Ocean CO_2 Uptake', *Global Biogeochem. Cycles* **7**, 353–368.

Tans, P. P., Fung, I. Y., and Takahashi, T.: 1990, 'Observational Constraints on the Global Atmospheric CO_2 Budget', *Science* **247**, 1431–1438.

Volk, T. and Liu, Z.: 1988, 'Controls of CO_2 Sources and Sinks in the Earth Scale Surface Ocean: Temperature and Nutrients', *Global Biogeochem. Cycles* **2**, 73–89.

Wigley, T. M. L.: 1993, 'Balancing the Carbon Budget. Implications for Projections of Future Carbon Dioxide Concentration Changes', *Tellus* **45B**, 409–425.

Wuebbles, D. J., Jain, A. K., Patten, K. O., and Grant, K. E.: 1995, 'Sensitivity of Direct Global Warming Potentials to Uncertainties', *Climatic Change* **29**, 265–297.

(Received 10 January 1995; in final form 4 December 1995)